Dinaphthothiepine Bisimide and Its Sulfoxide: Soluble Precursors for Perylene Bisimide

Sakiho Hayakawa,† Kyohei Matsuo,‡ Hiroko Yamada,*,‡ Norihito Fukui,*,† and Hiroshi Shinokubo*,†

† Department of Molecular and Macromolecular Chemistry, Graduate School of Engineering, Nagoya University, Furo-cho, Chikusa-ku, Nagoya, Aichi 464-8603, Japan

‡ Division of Materials Science, Graduate School of Science and Technology, Nara Institute of Science and Technology, 8916-5 Takayama-cho, Ikoma, Nara 630-0192, Japan

ABSTRACT: The synthesis and properties of dinaphtho[1,8-bc:1',8'-ef]thiepine bisimide (DNTBI) and its oxides are described. Their molecular design is conceptually based on the insertion of a sulfur atom into the perylene bisimide (PBI) core. These sulfur-inserted PBI derivatives adopt nonplanar structures, which significantly increases their solubility in common organic solvents. Upon electron-injection, light-irradiation, or heating, DNTBI and its sulfoxides undergo sulfur-extrusion reactions to furnish PBI. The photo-induced and thermal sulfur extrusion reactions proceed almost quantitatively. This unique reactivity enabled the fabrication of a high-performance solution-processed n-type organic field-effect transistor with an electron mobility of up to 0.41 $cm^2 V^{-1} s^{-1}$.

Organic semiconductors are key components in organic electronic and optoelectronic devices.[1–5] The use of organic materials as semiconductors is potentially advantageous considering that large devices can be fabricated at low cost and/or low temperature based on solution processes. However, high-performance semiconducting molecules often exhibit low solubility in organic solvents. The use of soluble precursors, which provide the corresponding semiconducting molecules upon appropriate external stimuli such as heat and light, is a promising approach to solve this issue (Figure 1).[6–9] Furthermore, such soluble precursors are versatile because they allow the generation of sophisticated morphologies.[10] For p-type organic semiconductors, a wide range of soluble precursors has been developed.[6–15] In contrast, comparable soluble precursors for n-type semiconductors remain elusive and would thus represent highly attractive research targets.[16–21] In addition, the development of new design guidelines for soluble precursors should be important as current strategies rely mainly on three approaches: retro-Diels–Alder reactions, decarbonylative aromatizations, and thermal removal of peripherally attached *tert*-butoxycarbonyl groups.

Perylene bisimide (PBI) is a promising prospective n-type organic semiconductor.[22–32] However, the current design guidelines for soluble precursors are not suitable for PBI owing to the following two reasons: i) PBI does not contain a suitable six-membered ring for retro-Diels–Alder reactions or decarbonylative aromatizations; ii) thermal removal of *tert*-butoxycarbonyl groups from imide-nitrogens affords only hydrogen-substituted PBIs, despite the importance of imide-substituents to control the solid-state molecular arrangement, electron mobility, and device stability. Therefore, the development of a different strategy is essential for the design of versatile PBI precursors.

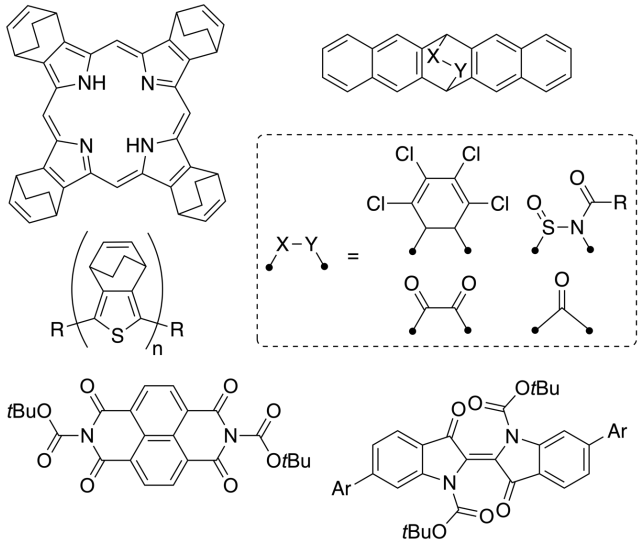

Figure 1. Soluble precursors for organic semiconductors.

Several organosulfur compounds are susceptible to sulfur-extrusion reactions (Figure 2).[33–45] For example, thiepine undergoes 6π-electrocyclization even at –70 °C to afford thianorcaradiene, which provides benzene from subsequent intermolecular collisions (eq.1).[41–44] Wolf and co-workers have reported that photo-irradiation of 9-to-9' sulfoxide-bridged anthracene dimer results in a rapid loss of the bridging SO unit to afford 9,9'-bianthracene (eq. 2).[45] Consequently, organosulfur compounds could potentially serve as soluble precursors for π-systems via sulfur-extrusion. Besides, our group has reported that the conceptual insertion of a nitrogen atom represents an effective strategy to create nonplanar and soluble PBI analogues.[46] Herein, we report the synthesis and properties of dinaphtho[1,8-bc:1',8'-ef]thiepine bisimide (DNTBI) and its oxides

as soluble precursors for PBI (eq.3). Notably, these precursors underwent photo-induced and thermal sulfur extrusion reactions almost quantitatively, enabling the fabrication of a high-performance solution-processed n-type organic field-effect transistor. Such dual stimuli-responsibility has been limited to norbornadienone derivatives among soluble precursors for organic semiconductors.[6–9]

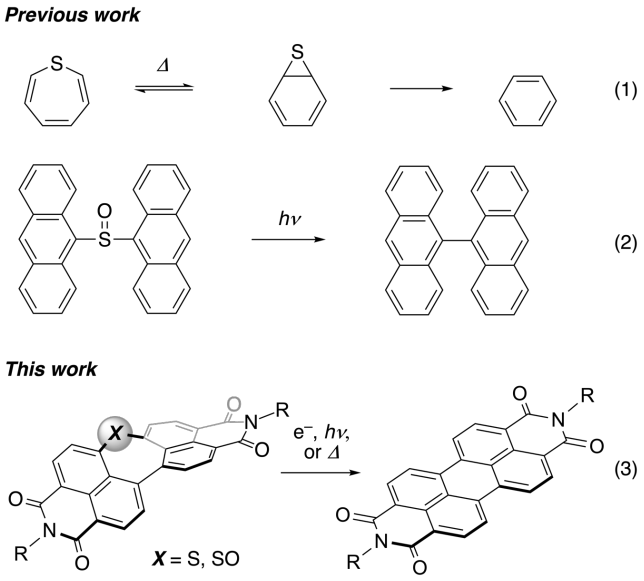

Figure 2. Sulfur-extrusion reactions.

The synthesis of DNTBIs as well as the corresponding sulfoxides and sulfones is shown in Scheme 1. The nucleophilic aromatic substitution of brominated naphthalene monoimide dimers[46] **1a** (R = C_8H_{17}) and **1b** (R = C_4H_9) with sodium sulfide afforded DNTBIs **2a** and **2b** in 47% and 48% yield, respectively. The molecular structure of **2b** was unambiguously determined by a single-crystal X-ray diffraction analysis (Figure 3). DNTBI **2b** shows a bent structure, in which the sulfur atom protrudes from the π-surface. Such a distorted conformation resembles that of a previously reported nitrogen-inserted PBI analogue.[46] Subsequently, **2a** and **2b** were oxidized with *m*-chloroperbenzoic acid (*m*CPBA, 1.0 equiv) to afford the corresponding sulfoxides **3a** and **3b** in 78% and 84% yield, respectively. Moreover, the tungsten-catalyzed oxidation[47] of **2a** and **2b** with hydrogen peroxide provided sulfones **4a** and **4b** in 95% and 85% yield, respectively.

DNTBI **2a**, sulfoxide **3a**, and sulfone **4a** are soluble in common organic solvents such as CH_2Cl_2, toluene, EtOAc, THF, and DMF. The solubility values (*S* g/100 g CH_2Cl_2) of **2a** (2.9), **3a** (0.51), and **4a** (5.4) are 150–1700 times higher than that of the parent PBI **5a** (3.3×10^{-3}) (Figure S19). The substantially high solubility of **2a**, **3a**, and **4a** is most likely due to their nonplanar structures.[48,49]

Scheme 1. Syntheses of DNTBIs and their oxides

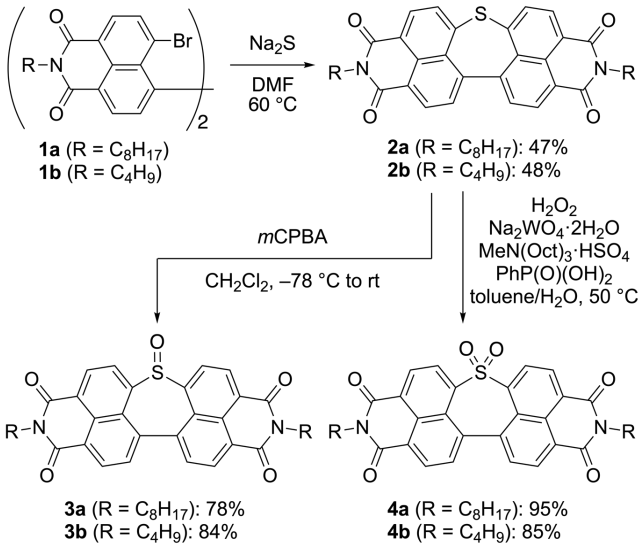

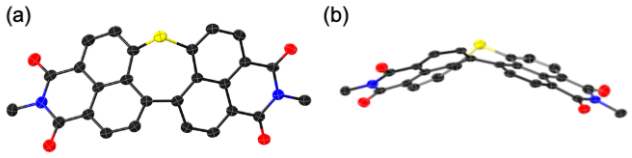

Figure 3. X-ray crystal structure of **2b**. (a) Top and (b) side views. Thermal ellipsoids at 50% probability. All hydrogen atoms and propyl groups omitted for clarity.

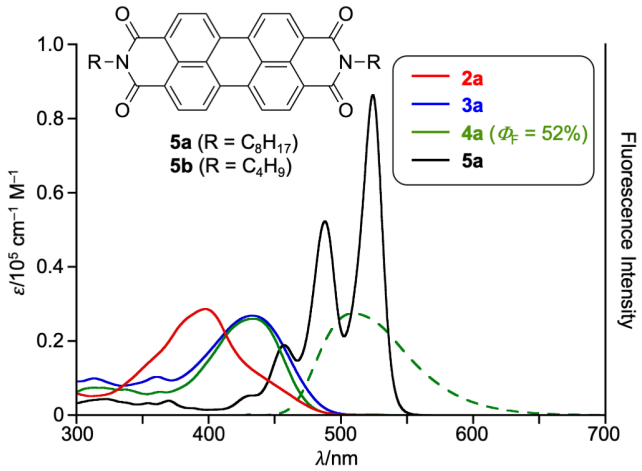

Figure 4. UV/vis absorption spectra of **2a**, **3a**, **4a**, and **5a** (solid lines) and fluorescence spectrum of **4a** (green dashed line) in CH_2Cl_2. λ: wavelength, ε: extinction coefficient.

The UV/vis absorption spectra of **2a**, **3a**, **4a**, and PBI **5a** as well as the emission spectrum of **4a** are shown in Figure 4. The absorption spectra of **2a**, **3a**, and **4a** are hypsochromically shifted relative to that of **5a**, which can be attributed to the disrupted conjugation around the inserted sulfur atom. DNTBI **2a** exhibited an absorption maximum at 397 nm together with a weak absorption between 420 and 500 nm, whose spectral features resemble that of the aforementioned nitrogen-inserted PBI analogue.[46] Sulfoxide **3a** and sulfone **4a** displayed absorption maxima at 433 and 434 nm, respectively, which are substantially red-shifted relative to that of **2a**. Sulfone **4a** exhibited green emission at 510 nm with a moderate fluorescence

quantum yield (Φ_F = 52%). The emission spectra of **2a** and **3a** were not recorded due to the formation of PBI **5a** upon photoexcitation (*vide infra*).

Scheme 2. Reduction of DNTBI 2a and sulfoxide 3a

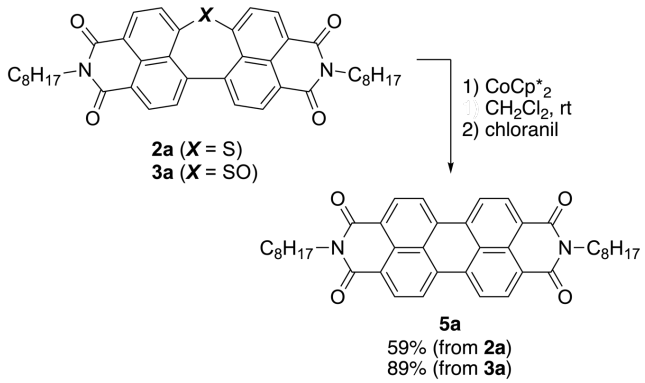

We examined the sulfur-extrusion reactions by electron-injection. Treatment of **2a** and **3a** with decamethylcobaltocene ($CoCp^*_2$) followed by quenching with chloranil afforded PBI **5a** in 59% and 89% yield, respectively (Scheme 2). The generation of PBI **5a** was also triggered by electrochemical reduction as proven by cyclic voltammetry (Figure S20) and spectroelectrochemical measurements (Figure S26–29). The results of density functional theory (DFT) calculations suggested that the radical anion of **2a** exhibits a shortened C–C distance (2.716 Å) between the two *α*-carbons of the central sulfur atom compared to that of the neutral form (2.871 Å) (Figure S24). Furthermore, an isomerization pathway from the radical anion to a thianorcaradiene-like species seems feasible (Figure S25). This intermediate would most likely engage in intermolecular collisions to provide the radical anion of PBI, which is similar to a pathway that has been proposed for the extrusion of sulfur from thiepine (Figure 2, eq. 1).[41–44]

We monitored the changes in the absorption spectra of DNTBI **2a** and sulfoxide **3a** upon photo-irradiation (Figure 5). The experiments were conducted under an N_2 atmosphere and the solvent (CH_2Cl_2) was degassed by N_2 sparging. The photo-irradiation was performed by a high-pressure mercury lamp equipped with a sharp cut filter ($\lambda > 380$ nm). Interestingly, the characteristic absorption of PBI **5a** gradually appeared between 450 and 550 nm, accompanied by clear isosbestic points. The absorption spectra after photo-irradiation for 1200 s are almost identical to that of **5a**, indicating a nearly quantitative conversion. The reaction of **3a** is faster than that of **2a**. The photo-induced generation of PBI **5a** from **2a** and **3a** was also confirmed by a ^{1}H NMR analysis (Figures S30,31). In contrast, sulfone **4a** shows no distinct change upon irradiation (Figure S32). The photo-induced sulfur-extrusion reactions of **2a** and **3a** can be retarded by sparging with air (Figure S33a). A similar result was observed for 9-to-9' sulfone-bridged anthracene dimer.[45] These results may suggest the possible involvement of a triplet state species as an intermediate. It is also worth noting that the reaction rate is virtually independent on the solvent polarity, implying that the formation of charge-transfer states does not play an important role (Figure S33b).

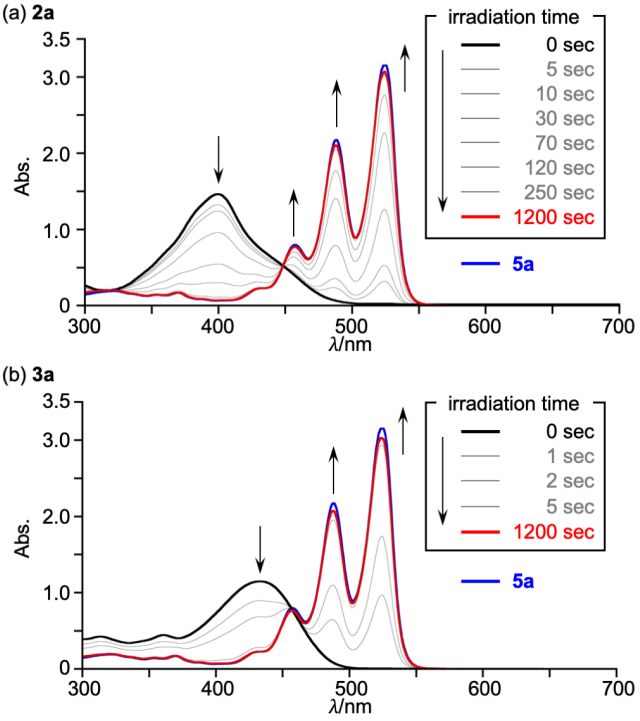

Figure 5. Changes in the UV/vis absorption spectra of **2a** and **3a** upon photo-irradiation in CH_2Cl_2 under an N_2 atmosphere. For the photo-irradiation, a high-pressure mercury lamp equipped with a sharp cut filter ($\lambda > 380$ nm) was employed. $[\mathbf{2a}]_0 = [\mathbf{3a}]_0 = [\mathbf{5a}] = 4.2 \times 10^{-5}$ M^{-1}.

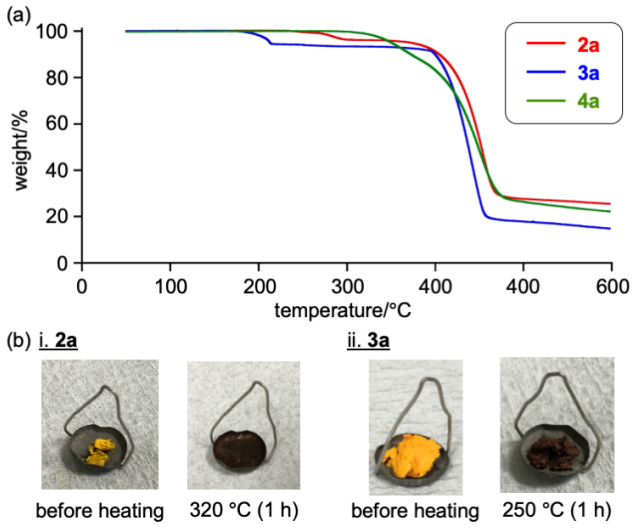

Figure 6. (a) TGA profiles of **2a**, **3a**, and **4a**; heating gradient: 5.0 °C min^{-1}. (b) Solid samples of (i) **2a** and (ii) **3a** before and after heating.

To examine the effect of heating on the sulfur-extrusion reactions, thermogravimetric analyses (TGA) were conducted on **2a**, **3a**, and **4a** (Figure 6). The TGA profiles of DNTBI **2a** and sulfoxide **3a** exhibited mass decreases of 4% and 6% at 300 and 225 °C, respectively, which agrees well with the expected changes for the formation of PBI. In contrast, the TGA profile of sulfone **4a** showed a weight loss of ca. 70% around 400 °C, indicating thermal decomposition. The ^{1}H NMR and thin-layer chromatography analyses of the brown samples formed upon heating **2a** and **3a** indicate an almost quantitative formation of PBI (Figure S35,36). It is worth noting that heating crystalline solids of **2a** for 1 h at 300 °C provided a waxy PBI solid (Figure

6b and S34a). Considering that the melting point of PBI **5a** is higher than 350 °C, this change of solid morphology by heating indicates that the sulfur-extrusion reaction of **2a** proceeds after melting. Conversely, the solid sample of **3a** remained crystalline even after heating to 250 °C for 1 h (Figure S34b). Its powder X-ray diffraction pattern was identical to that of PBI **5a** (Figure S37). In addition, the progress of thermal conversion for the spin-coated film of **3a** on a glass substrate at 230 °C was monitored by measuring the UV/vis absorption spectra, which indicates that the sulfur-extrusion reaction was completed within 2 min and the further annealing caused no apparent degradation (Figure S38). We also examined the cooperative effect of light and heat for the conversion of crystalline samples of sulfoxide **3a** to PBI **5a** (Figure S44). At 140 °C, photoirradiation slightly increased the amount of PBI. These preliminary results are promising for the creation of flexible devices with PEN or PET substrates.

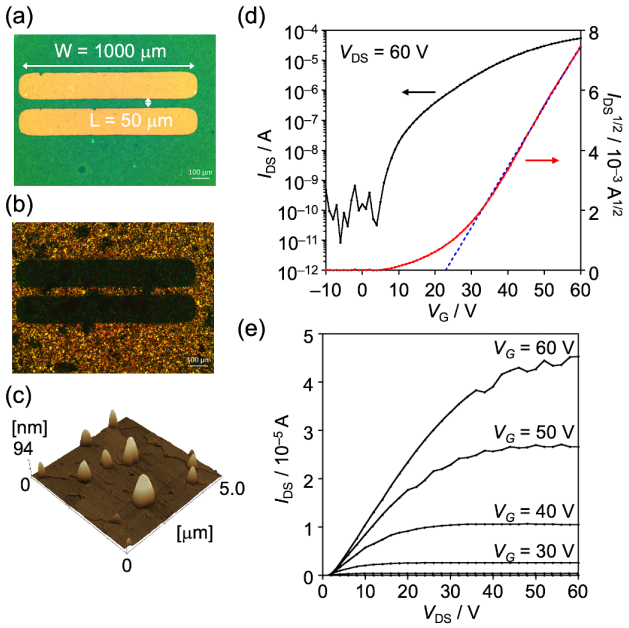

Figure 7. Morphologies and FET properties of a spin-cast film of **3a** after heating. (a) Optical micrograph. (b) Polarization optical micrograph. (c) AFM image. (d) Transfer characteristics. (e) Output characteristics.

Bottom-gate top-contact field-effect transistor (FET) devices were fabricated (Figures 7 and S39–43). The substrate surface was modified with a self-assembled monolayer of 12-cyclohexyldodecylphosphonic acid (CDPA) on an Al_2O_3/SiO_2 dielectric layer.[50] A $CHCl_3$ solution of sulfoxide **3a** (5 g L^{-1}) was spin-coated on the substrate (30 s; 2000 rpm). The substrate was heated at 230 °C for 5 min under a nitrogen atmosphere to cause the extrusion of sulfur. Gold electrodes were vacuum-deposited on the active layer as source and drain electrodes. Subsequently, OFET properties were measured at ambient temperature under vacuum conditions (> 2×10^{-1} Pa). The obtained OFETs exhibited typical n-type behavior. The average and maximum electron mobilities μ_e are 0.13 and 0.41 cm^2 V^{-1} s^{-1}, respectively, with a threshold voltage V_{th} of 23 V and an on/off current ratio I_{on}/I_{off} of 3×10^5. The small hysteresis is observed in the transfer characteristic (Figure S41). These mobilities are comparable to that of the vacuum-deposited film of **5a** (μ_e = 0.6 cm^2 V^{-1} s^{-1}).[51] A polarized optical microscopy analysis indicated that this spin-coated film is polycrystalline. The XRD pattern of this film exhibited a distinct peak due to *d*-spacing of 21.6 Å (Figure S40), which is comparable to that of the vacuum-deposited film (*d*-spacing = 20.3 Å) and the XRD pattern predicted from the crystal structure of **5a** (*d*-spacing = 19.6 Å). The difference of surface morphologies before and after thermal conversion was examined by atomic force microscopy (AFM). While the surface before heating was very smooth, relatively rough surface with several grains was observed after heating probably due to the release of gas during sulfur-extrusion reaction and/or the crystallization of PBI (Figure 7c). The root mean square (RMS) roughness value was calculated to be 16.1 nm. Further examinations, especially the effect of photo-conversion and development of a reliable procedure with high reproductivity, are actively underway in our groups.

In summary, we have synthesized dinaphtho[1,8-bc:1',8'-ef]thiepine bisimides (DNTBIs) **2a,b** as well as the corresponding sulfoxides **3a,b** and sulfones **4a,b**. The molecular design is based on the insertion of a sulfur atom into a perylene bisimide (PBI) core. A single-crystal X-ray diffraction analysis confirmed that DNTBI **2b** adopts a nonplanar structure owing to the embedded seven-membered ring. The distorted conformation endows these sulfur-containing PBI analogues with excellent solubility. Notably, DNTBI **2a** and sulfoxide **3a** undergo sulfur-extrusion reactions upon electron-injection, light-irradiation, or heating. In particular, the light- and heat-induced sulfur-extrusion reactions proceed almost quantitatively. These features enable the fabrication of a high-performance organic FET with the electron mobility of up to 0.41 cm^2 V^{-1} s^{-1}.

ASSOCIATED CONTENT

Supporting Information

The Supporting Information is available free of charge on the ACS Publications website.
Experimental details and spectral data for all new compounds.
Crystallographic data (CIF files) for **3b**.

AUTHOR INFORMATION

Corresponding Author

hyamada@ms.naist.jp, fukui@chembio.nagoya-u.ac.jp, hshino@chembio.nagoya-u.ac.jp

Funding Sources

The authors declare the absence of any potentially competing financial interests.

ACKNOWLEDGMENT

This work was supported by JSPS KAKENHI grant JP17H01190 and JP20K15257. H.S. thanks the Sumitomo Foundation for financial support. N.F. gratefully acknowledges the Tatematsu Foundation and Iketani Science and Technology Foundation for financial support. We thank Prof. Masami Kamigaito and Dr. Mineto Uchiyama (Nagoya University) for thermogravimetric analyses. We thank Prof. Yukihatu Uraoka, Dr. Mutsunori Uenuma, Dr. Takuya Okabe (NAIST), and Prof. Mitsuharu Suzuki (Osaka University) for the frequency-dependent capacitance measurements of dielectric layer.

REFERENCES

(1) Wang, C.; Dong, H.; Hu, W.; Liu, Y.; Zhu, D. Semiconducting π-Conjugated Systems in Field-Effect Transistors: A Material Odyssey of Organic Electronics. *Chem. Rev.* **2012**, *112*, 2208–2267.

(2) Jones, B. A.; Ahrens, M. J.; Yoon, M.-H.; Facchetti, A.; Marks, T. J.; Wasielewski, M. R. High-Mobility Air-Stable n-Type Semiconductors with Processing Versatility: Dicyanoperylene-3,4:9,10-bis(dicarboximides). *Angew. Chem., Int. Ed.* **2004**, *43*, 6363–6366.

(3) Facchetti, A.; Yoon, M.-H.; Stern, C. L.; Hutchison, G. R.; Ratner, M. A.; Marks, T. J. Building Blocks for N-Type Molecular and Polymeric Electronics. Perfluoroalkyl- versus Alkyl-Functionalized Oligothiophenes (nTs; n = 2–6). Systematic Synthesis, Spectroscopy, Electrochemistry, and Solid-State Organization. *J. Am. Chem. Soc.* **2004**, *126*, 13480–13501.

(4) Yoon, M.-H.; DiBenedetto, S. A.; Russell, M. T.; Facchetti, A.; Marks, T. J. High-Performance n-Channel Carbonyl-Functionalized Quaterthiophene Semiconductors; Thin-Film Transistor Response and Majority Carrier Type Inversion via Simple Chemical Protection/Deprotection. *Chem. Mater.* **2007**, *19*, 4864–4881.

(5) Mu, C.; Liu, P.; Ma, W.; Jiang, K.; Zhao, J.; Zhang, K.; Chen, Z.; Wei, Z.; Yi, Y.; Wang, J.; Yang, S.; Huang, F.; Facchetti, A.; Ade, H.; Yan, H. High-Efficiency All-Polymer Solar Cells Based on a Pair of Crystalline Low-Bandgap Polymers. *Adv. Mater.* **2014**, *26*, 7224–7230.

(6) Yamada, H.; Okujima, T.; Ono, N. Organic Semiconductors Based on Small Molecules with Thermally or Photochemically Removable Groups. *Chem. Commun.* **2008**, 2957.

(7) Mei, J.; Diao, Y.; Appleton, A. L.; Fang, L.; Bao, Z. Integrated Materials Design of Organic Semiconductors for Field-Effect Transistors. *J. Am. Chem. Soc.* **2013**, *135*, 6724–6746.

(8) Watanabe, M.; Chen, K.-Y.; Chang, Y. J.; Chow, T. J. Acenes Generated from Precursors and Their Semiconducting Properties. *Acc. Chem. Res.* **2013**, *46*, 1606–1615.

(9) Freudenberg, J.; Jänsch, D.; Hinkel, F.; Bunz, U. H. F. Immobilization Strategies for Organic Semiconducting Conjugated Polymers. *Chem. Rev.* **2018**, *118*, 5598–5689.

(10) Matsuo, Y.; Sato, Y.; Niinomi, T.; Soga, I.; Tanaka, H.; Nakamura, E. Columnar Structure in Bulk Heterojunction in Solution-Processable Three-Layered p-i-n Organic Photovoltaic Devices Using Tetrabenzoporphyrin Precursor and Silylmethyl[60]Fullerene. *J. Am. Chem. Soc.* **2009**, *131*, 16048–16050.

(11) Herwig, P. T.; Müllen, K. A Soluble Pentacene Precursor: Synthesis, Solid-State Conversion into Pentacene and Application in a Field-Effect Transistor. *Adv. Mater.* **1999**, *11*, 480–483.

(12) Afzali, A.; Dimitrakopoulos, C. D.; Breen, T. L. High-Performance, Solution-Processed Organic Thin Film Transistors from a Novel Pentacene Precursor. *J. Am. Chem. Soc.* **2002**, *124*, 8812–8813.

(13) Aramaki, S.; Sakai, Y.; Ono, N. Solution-Processible Organic Semiconductor for Transistor Applications: Tetrabenzoporphyrin. *Appl. Phys. Lett.* **2004**, *84*, 2085–2087.

(14) Nakayama, K.; Ohashi, C.; Oikawa, Y.; Motoyama, T.; Yamada, H. Characterization and Field-Effect Transistor Performance of Printed Pentacene Films Prepared by Photoconversion of a Soluble Precursor. *J. Mater. Chem. C* **2013**, *1*, 6244.

(15) Liu, J.; Kadnikova, E. N.; Liu, Y.; McGehee, M. D.; Fréchet, J. M. J. Polythiophene Containing Thermally Removable Solubilizing Groups Enhances the Interface and the Performance of Polymer−Titania Hybrid Solar Cells. *J. Am. Chem. Soc.* **2004**, *126*, 9486–9487.

(16) Zambounis, J. S.; Hao, Z.; Iqbal, A. Latent Pigments Activated by Heat. *Nature* **1997**, *388*, 131–132.

(17) Petersen, M. H.; Gevorgyan, S. A.; Krebs, F. C. Thermocleavable Low Band Gap Polymers and Solar Cells Therefrom with Remarkable Stability toward Oxygen. *Macromolecules* **2008**, *41*, 8986–8994.

(18) Głowacki, E. D.; Apaydin, D. H.; Bozkurt, Z.; Monkowius, U.; Demirak, K.; Tordin, E.; Himmelsbach, M.; Schwarzinger, C.; Burian, M.; Lechner, R. T.; Demitri, N.; Voss, G.; Sariciftci, N. S. Air-Stable Organic Semiconductors Based on 6,6′-Dithienylindigo and Polymers Thereof. *J. Mater. Chem. C* **2014**, *2*, 8089–8097.

(19) Guo, C.; Quinn, J.; Sun, B.; Li, Y. An Indigo-Based Polymer Bearing Thermocleavable Side Chains for n-Type Organic Thin Film Transistors. *J. Mater. Chem. C* **2015**, *3*, 5226–5232.

(20) Liu, C.; Dong, S.; Cai, P.; Liu, P.; Liu, S.; Chen, J.; Liu, F.; Ying, L.; Russell, T. P.; Huang, F.; Cao, Y. Donor–Acceptor Copolymers Based on Thermally Cleavable Indigo, Isoindigo, and DPP Units: Synthesis, Field Effect Transistors, and Polymer Solar Cells. *ACS Appl. Mater. Interfaces* **2015**, *7*, 9038–9051.

(21) Nakamura, T.; Shioya, N.; Shimoaka, T.; Nishikubo, R.; Hasegawa, T.; Saeki, A.; Murata, Y.; Murdey, R.; Wakamiya, A. Molecular Orientation Change in Naphthalene Diimide Thin Films Induced by Removal of Thermally Cleavable Substituents. *Chem. Mater.* **2019**, *31*, 1729–1737.

(22) Weil, T.; Vosch, T.; Hofkens, J.; Peneva, K.; Müllen, K. The Rylene Colorant Family-Tailored Nanoemitters for Photonics Research and Applications. *Angew. Chem., Int. Ed.* **2010**, *49*, 9068–9093.

(23) Würthner, F.; Saha-Möller, C. R.; Fimmel, B.; Ogi, S.; Leowanawat, P.; Schmidt, D. Perylene Bisimide Dye Assemblies as Archetype Functional Supramolecular Materials. *Chem. Rev.* **2016**, *116*, 962–1052.

(24) Würthner, F.; Stolte, M. Naphthalene and Perylene Diimides for Organic Transistors. *Chem. Commun.* **2011**, *47*, 5109.

(25) Zhan, X.; Facchetti, A.; Barlow, S.; Marks, T. J.; Ratner, M. A.; Wasielewski, M. R.; Marder, S. R. Rylene and Related Diimides for Organic Electronics. *Adv. Mater.* **2011**, *23*, 268–284.

(26) Huang, C.; Barlow, S.; Marder, S. R. Perylene-3,4,9,10-Tetracarboxylic Acid Diimides: Synthesis, Physical Properties, and Use in Organic Electronics. *J. Org. Chem.* **2011**, *76*, 2386–2407.

(27) Wang, C.; Dong, H.; Hu, W.; Liu, Y.; Zhu, D. Semiconducting π-Conjugated Systems in Field-Effect Transistors: A Material Odyssey of Organic Electronics. *Chem. Rev.* **2012**, *112*, 2208–2267.

(28) Liu, Z.; Zhang, G.; Cai, Z.; Chen, X.; Luo, H.; Li, Y.; Wang, J.; Zhang, D. New Organic Semiconductors with Imide/Amide-Containing Molecular Systems. *Adv. Mater.* **2014**, *26*, 6965–6977.

(29) Horowitz, G.; Kouki, F.; Spearman, P.; Fichou, D.; Nogues, C.; Pan, X.; Garnier, F. Evidence for N-Type Conduction in a Perylene Tetracarboxylic Diimide Derivative. *Adv. Mater.* **1996**, *8*, 242–245.

(30) Ostrick, J. R.; Dodabalapur, A.; Torsi, L.; Lovinger, A. J.; Kwock, E. W.; Miller, T. M.; Galvin, M.; Berggren, M.; Katz, H. E. Conductivity-Type Anisotropy in Molecular Solids. *J. Appl. Phys.* **1997**, *81*, 6804–6808.

(31) Struijk, C. W.; Sieval, A. B.; Dakhorst, J. E. J.; van Dijk, M.; Kimkes, P.; Koehorst, R. B. M.; Donker, H.; Schaafsma, T. J.; Picken, S. J.; van de Craats, A. M.; Warman, J. M.; Zuilhof, H.; Sudhölter, E. J. Liquid Crystalline Perylene Diimides: Architecture and Charge Carrier Mobilities. *J. Am. Chem. Soc.* **2000**, *122*, 11057–11066.

(32) Schmidt, R.; Oh, J. H.; Sun, Y.-S.; Deppisch, M.; Krause, A.-M.; Radacki, K.; Braunschweig, H.; Könemann, M.; Erk, P.; Bao, Z.; Würthner, F. High-Performance Air-Stable n-Channel Organic Thin Film Transistors Based on Halogenated Perylene Bisimide Semiconductors. *J. Am. Chem. Soc.* **2009**, *131*, 6215–6228.

(33) Taylor, R. J. K. Recent Developments in Ramberg–Bäcklund and Episulfone Chemistry. *Chem. Commun.* **1999**, 217–227.

(34) Boekelheide, V.; Reingold, I. D.; Tuttle, M. Syntheses of Cyclophanes by Photochemical Extrusion of Sulphur. *J. Chem. Soc. Chem. Commun.* **1973**, 406.

(35) Givens, R. S.; Olsen, R. J.; Wylie, P. L. Photoextrusion of Sulfur Dioxide: General Route to [2.2]Cyclophanes. *J. Org. Chem.* **1979**, *44*, 1608–1613.

(36) Armarego, W. L. F. The Synthesis of Two Dinaphthothiophens. *J. Chem. Soc.* **1960**, 433–436.

(37) Schroth, W.; Hintzsche, E.; Felicetti, M.; Spitzner, R.; Sieler, J.; Kempe, R. Concerning the Questionable Existence of Thioxoindigoid Compounds. *Angew. Chem., Int. Ed. Engl.* **1994**, *33*, 739–741.

(38) Wakamiya, A.; Nishinaga, T.; Komatsu, K. 1,2-Dithiin Annelated with Bicyclo[2.2.2]Octene Frameworks. One-Electron and Two-Electron Oxidations and Formation of a Novel 2,3,5,6-Tetrathiabicyclo[2.2.2]Oct-7-Ene Radical Cation with Remarkable Stability Owing to a Strong Transannular Interaction. *J. Am. Chem. Soc.* **2002**, *124*, 15038–15050.

(39) Okamoto, T.; Kudoh, K.; Wakamiya, A.; Yamaguchi, S. General Synthesis of Thiophene and Selenophene-Based Heteroacenes. *Org. Lett.* **2005**, *7*, 5301–5304.

(40) Kamiya, H.; Kondo, T.; Sakida, T.; Yamaguchi, S.; Shinokubo, H. *meso*-Thiaporphyrinoids Revisited: Missing of Sulfur by Small Metals. *Chem.-Eur. J.* **2012**, *18*, 16129–16135.

(41) Hoffman, J. Matthew.; Schlessinger, R. H. Synthesis of a Stable 8-π-Electron Thiepin. *J. Am. Chem. Soc.* **1970**, *92*, 5263–5265.

(42) Barton, T. J.; Martz, M. D.; Zika, R. G. Facile Bridge Expulsion of Sulfur Heterocycles. 7-Thiabicyclo[2.2.1]Hepta-2,5-Diene and 7-Thiabicyclo[4.1.0]Hepta-2,4-Diene Systems in Thiepin Synthesis. *J. Org. Chem.* **1972**, *37*, 552–554.

(43) Nishino, K.; Yano, S.; Kohashi, Y.; Yamamoto, K.; Murata, I. Synthesis of 2,7-Di-Tert-Butyl-4-Ethoxycarbonyl-5-Methylthiepin. A Remarkably Stable and Simple Monocyclic Thiepin. *J. Am. Chem. Soc.* **1979**, *101*, 5059–5060.

(44) Gleiter, R.; Krennrich, G.; Cremer, D.; Yamamoto, K.; Murata, I. Electronic Structure and Thermal Stability of Thiepins. Photoelectron Spectroscopic Investigations. *J. Am. Chem. Soc.* **1985**, *107*, 6874–6879.

(45) Christensen, P. R.; Patrick, B. O.; Caron, É.; Wolf, M. O. Oxidation-State-Dependent Photochemistry of Sulfur-Bridged Anthracenes. *Angew. Chem., Int. Ed.* **2013**, *52*, 12946–12950.

(46) Hayakawa, S.; Kawasaki, A.; Hong, Y.; Uraguchi, D.; Ooi, T.; Kim, D.; Akutagawa, T.; Fukui, N.; Shinokubo, H. Inserting Nitrogen: An Effective Concept To Create Nonplanar and Stimuli-Responsive Perylene Bisimide Analogues. *J. Am. Chem. Soc.* **2019**, *141*, 19807–19816.

(47) Sato, K.; Hyodo, M.; Aoki, M.; Zheng, X.-Q.; Noyori, R. Oxidation of Sulfides to Sulfoxides and Sulfones with 30% Hydrogen Peroxide under Organic Solvent- and Halogen-Free Conditions. *Tetrahedron* **2001**, *57*, 2469–2476.

(48) Kawasumi, K.; Zhang, Q.; Segawa, Y.; Scott, L. T.; Itami, K. A Grossly Warped Nanographene and the Consequences of Multiple Odd-Membered-Ring Defects. *Nat. Chem.* **2013**, *5*, 739–744.

(49) Fukui, N.; Kim, T.; Kim, D.; Osuka, A. Porphyrin Arch-Tapes: Synthesis, Contorted Structures, and Full Conjugation. *J. Am. Chem. Soc.* **2017**, *139*, 9075–9088.

(50) Liu, D.; He, Z.; Su, Y.; Diao, Y.; Mannsfeld, S. C. B.; Bao, Z.; Xu, J.; Miao, Q. Self-Assembled Monolayers of Cyclohexyl-Terminated Phosphonic Acids as a General Dielectric Surface for High-Performance Organic Thin-Film Transistors. *Adv. Mater.* **2014**, *26*, 7190–7196.

(51) Chesterfield, R. J.; McKeen, J. C.; Newman, C. R.; Ewbank, P. C.; da Silva Filho, D. A.; Brédas, J.-L.; Miller, L. L.; Mann, K. R.; Frisbie, C. D. Organic Thin Film Transistors Based on *N*-Alkyl Perylene Diimides: Charge Transport Kinetics as a Function of Gate Voltage and Temperature. *J. Phys. Chem. B* **2004**, *108*, 19281–19292.

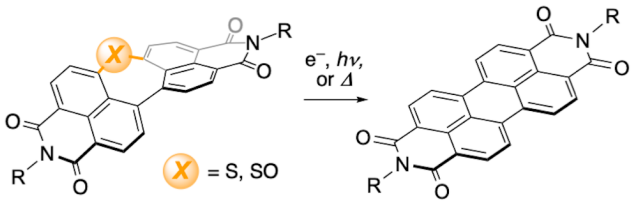

DNTBI and its sulfoxide **PBI**

solution-processed OFET (μ = 0.41 cm^2 V^{-1} s^{-1})